XRPD study of the metoprolol fumarate salt: crystal structure and anisotropic thermal expansion. Comparison with the analogous tartrate and succinate salts.

Patrizia Rossi,[a] Paola Paoli,[a,*] Laura Chelazzi,[b] Luca Conti,[c] Andrea Bencini[c]

[a] = Department of Industrial Engineering, University of Florence (Italy). [b] = Centro di Cristallografia Strutturale, University of Florence (Italy). [c] = Department of Chemistry "Ugo Schiff", University of Florence (Italy) * = paola.paoli@unifi.it

Keywords: metoprolol fumarate, XRPD structure solution, anisotropic lattice expansion, VT-XRPD, Graph Sets and Hirshfeld Surfaces analyses.

Abstract: The metoprolol fumarate (**MF**) salt has been characterized by a combined use of X-ray powder diffraction (XRPD), variable temperature XRPD (VT-XRPD) and differential scanning calorimetry (DSC). Its molecular and crystal structure, as determined from XRPD data, has been thoroughly compared to those of the analogous tartrate (**MT-o**) and succinate (**MS-m**) salts. Moreover Hirshfeld Surface Analysis and Graph Sets Analysis have been performed to achieve insights into the intermolecular interactions. Despite their evident similarities at the atomic level the three salts behave differently upon temperature variation: **MF** expands/contracts anisotropically (as **MS-m**), but the melt takes three days to recover the starting crystalline phase (as **MT-o**). A rationale for this behavior is provided based on their crystal arrangements.

Introduction

X-ray diffraction (XRD), both from single crystal (SCXRD) and microcrystalline powder (XRPD), has been often referred to as the gold standard in the characterization of solid state materials, as for example active pharmaceutical ingredients (API, including their salts, co-crystals, solvates and formulations).[1,2]

SCXRD allows to determine the molecular and crystalline structure and provides valuable information on conformational preferences, unusual molecular and crystal motifs, intermolecular interactions, H-bonding, etc.[3,4] However, SCXRD has an intrinsic limitation, that is the obtainment of single crystals of appropriate size and quality; when this condition is not fulfilled powder diffraction from microcrystalline powders can be a viable alternative. Commonly used for fingerprinting, as well as for quantitative phase analysis, XRPD patterns, due to diffraction peaks overlapping, usually provide much less structural details and definitely less accurate than SCXRD.

However, in recent years structure solution from powder diffraction has become a real opportunity,[5] while it is still not routine (in the Cambridge Structural Database[6] structures from powder diffraction data today represent the 0.5%).[7]

A crystal structure is a gold mine of information, which can greatly contribute to elucidate chemical/physical properties (structure-property relationships) of the solid state and, when complemented by data from Variable Temperature-XRPD (VT-XRPD) and Differential Scanning Calorimetry (DSC) to study thermally-induced phase transformations, provides an almost complete picture of the solid forms.[8,9,10,11]

In this paper the molecular and crystal structure of the metoprolol fumarate salt (**MF**, hereafter), as obtained from XRPD data, is reported together with a comparison with those of the strictly related tartrate and succinate salts (*vide infra*). Metoprolol, (±)-1-isopropylamino-3-[4-(2-methoxy-ethyl)-phenoxy]-prop- an-2-ol (Scheme 1), is a β_1 receptor blocker[12] with a wide range of medical indications (e.g. acute myocardial infarction, heart failure, angina pectoris, hypertension, etc.).[13,14] The molecule possesses a chiral center and, despite the β_1 blocking activity resides in the S-enantiomer,[15] it is usually manufactured as racemic mixture. In addition, due to its quite low melting point (323K),[16] metoprolol is always sold in salt-based formulations usually as tartrate, succinate or fumarate salts which differ for the release modalities.[17]

Recently[4] we have reported on the solid state structure and behavior of the tartrate salt (**MT)** compared to the succinate one (**MS**). In particular the comparison concerned the orthorhombic polymorph of **MT** (**MT-o**, in the following)[18] and the monoclinic polymorph of **MS**[19] (**MS-m** in the following).[20,21] The study was performed by in silico and experimental techniques (SCXRD, XRPD/VT-XRPD and DSC) in different controlled conditions. **MT-o** and **MS-m** crystal lattices are very similar in terms of number, type and geometry of the H-bond interactions as well as crystal densities but, quite surprisingly, the two salts have different "macroscopic" behavior. In fact, **MT-o** expands/contracts isotropically, while **MS-m** undergoes a reversible anisotropic lattice expansion/contraction on changing the temperature. Furthermore, while the succinate salt once melted quickly reverts to the starting crystal form on cooling, the tartrate transforms to an amorphous solid, which takes 6 days to completely recrystallize to the initial phase. Actually, we were unable to provide a really convincing and satisfying reason for the different bulk behavior of **MT-o** and **MS-m**, given their close similarities at the molecular/crystal level. In other words, the question "what really makes the difference between the crystal samples of **MS- m** and **MT-o** and possibly account for their macroscopic different behavior"[4] did not find a definitive answer.

With this in mind, and considering the importance that in-depth studies of the solid state structure of

APIs have in order to better understanding their macroscopic behavior, we have turned our attention to the other metoprolol salt typically employed in drug products, *i.e.* the fumarate one. Moreover the fumarate is a C_4 dicarboxylic acid anion as the tartrate and succinate ones and it can act only as H-bond acceptor as the succinate anion, thus the study of the metoprolol fumarate salt could help to understand the role played by the counterion in these salts and to find a possible correlation between atomic and macroscopic properties.

Thus, similarities and/or differences both at the atomic (molecular/crystal) and bulk levels between **MF** and the strictly related metoprolol salts **MT-o**[4] and **MS-m**[4,19] have been assessed and discussed. The paper is organized with a molecular and crystal description of **MF** as obtained from XRPD data, followed by Graph Sets and Hirshfeld analyses[22,23] to identify motifs and contributions to the intermolecular contacts which hold together the crystal packing. Then VT-XRPD and DSC measures were carried out in order to explore thermally-induced changes in **MF**. Results have been discussed and compared to those previously obtained for **MT-o** and **MS-m**.

EXPERIMENTAL SECTION

Material and methods. The metoprolol fumarate salt was purchased from Sigma Aldrich (grade: primary reference standard; CAS number 119637-66-0) and used as received, due to the good powder quality.

X-ray Powder Diffraction (XRPD)

Structure Determination. For crystal lattice parameters and structure determination of **MF** high quality XRPD data were recorded in a 0.5 mm capillary at room temperature by using a Bruker New D8 Da Vinci diffractometer (Cu-Kα radiation, 40 kV x 40 mA), equipped with a Bruker LYNXEYE-XE detector, scanning range 2θ=3-60°, 0.01° increments of 2θ and a counting time of 2s/step. Unit cell parameters were found with the algorithm DICVOL.[24] The asymmetric unit contains one metoprolol cation and one half of a fumarate anion. Space group determination with Highscore plus resulted in space group $P2_1/c$ with Z = 4. The structure was solved by simulated annealing that runs with structure fragments, performed with EXPO2014[25] using as a model structure for the metoprolol cation that found in **MT-o**[4] and for the fumarate anion that found in the diammonium fumarate structure (CSD refcode = NARDEP[26]). Ten runs for simulated annealing trial were set, and a cooling rate (defined as the ratio Tn/Tn−1) of 0.95 was used. Best solutions were chosen for Rietveld refinements, which were performed with the software TOPAS.[27] A shifted Chebyshev function with 8 coefficients and a Pseudo-Voigt function were used to fit background and peak shape, respectively. A rigid body constraint was applied for structure refinement. All the

hydrogen atoms were fixed in calculated positions. Crystal data and refinement parameters are reported in Table 1. Figure S1 shows the experimental, calculated, and difference diffraction patterns.

Variable temperature (VT-XRPD) Experiments. Temperature-resolved experiments (performed in triplicates) were performed in air in the 300 - 430 K range with an Anton Paar HTK 1200N hot chamber mounted on a Panalytical XPERT PRO diffractometer (Cu-Kα radiation, 40 kV x 40 mA), equipped with the PIX-CEL solid state fast detector. Scanning range 2θ = 4–40° with a 8 s/step counting time and 0.03° increments of 2θ. The temperature variation rate was 10 K/min; when the target temperature was reached the sample was kept 10 min at that temperature before data collection.

Finally, cell parameters at different temperatures were obtained performing a Pawley fit with the software TOPAS.[27] Background coefficients and zero shift were refined at ambient temperature and fixed for the other diffraction patterns collected at different temperature. The obtained unit cell parameters are listed in Table 2.

Differential Scanning Calorimetry (DSC)

Differential Scanning Calorimetry (DSC) experiments were performed by using a Mettler Toledo DSC1 Excellence instrument. Measurements were run in aluminum pans with pinhole lids (mass samples ranges from 1 to 3 mg). Temperature and enthalpy calibration were done using indium as a standard. Melting point (T_m) and heat of fusion (ΔH) were determined by measurements in the 310-450-310K range. A linear heating rate of 5K/min was used. Experiments were performed in air. DSC peaks were analyzed using the STAR^e software.[28] The melting data were the average of two measurements, and standard errors were ±0.1 K for temperature and ±0.3 kJ/mol for enthalpy.

Computational Section. The Mercury software 3.10.2[29] was used to analyze the crystal packing arrangement; in particular Graph Sets routine was used to describe the hydrogen bond networks in **MF**, **MT-o** and **MS-m** salts.

CrystalExplorer17[23] was used to compute Hirshfeld surfaces (HS).[30] Directions and strengths of the intermolecular interactions which build up the crystal have been mapped onto the HSs by using the d_{norm} descriptor. HSs were generated with the high resolution default with d_{norm} mapped over the standard color scale. The associated 2D fingerprint plots were considered (the standard 0.6-2.6Å view of d_e vs d_i was used) to identify and compare different kind of interactions in order to further detail the intermolecular interactions in the crystal packing of **MF** and of the strictly related **MT-o** and **MS-m** salts.

RESULTS

Molecular Structure from X-Ray Powder Diffraction

The metoprolol fumarate salt crystallizes in the monoclinic crystal system, space group $P2_1/c$. The asymmetric unit contains one molecule of the metoprolol cation and one half of the fumarate anion, the whole anion being completed by a crystallographic inversion center (-x, -y+1, -z-2). In the following, the discussion will be focused on the pharmacologically active S isomer of metoprolol (Figure 1). The overall shape adopted by the metoprolol cation in **MF** is almost identical to that found in the strictly related succinate salt (**MS-m**),[19] as provided by the most important dihedral angles[31] defining the conformation of both the side chains (see Table 3) and, as a consequence, the two cations almost superimpose (Figure 2). In contrast, in **MT** (both **MT-o**[4] **and MT-m**[16,32]) the metoprolol cation shows a different overall shape mostly because of the different conformation about the C7-C8 bond (*trans* vs *gauche*), in addition the ^{i}Pr terminal group is also differently orientated (Table 3 and Figure 2). In particular, as for **MF**, the side arm bearing the isopropyl group adopts a *trans-trans-gauche$^{(-)}$-trans* conformation (*ttg$^-$t* in the following). A search in the Cambridge Structural Database (CSD, v. 5.39, May 2018)[6] for the molecular fragment sketched in Scheme 2a results in 6 compounds,[4,19,33,34,35,36] which, based on the conformation adopted by the chain bearing the isopropyl group,[37] can be classified in three different conformational families (Figure 3), as already pointed out.[4] In particular **MT-o** and JIRWIR (CSD refcode) show an elongated conformation (*all trans*, *aT*), while a folded arrangement characterizes the other cations (*ttg$^-$t*: **MF**, **MS-m**, CIMJUD; *ttg$^+$t*: DETHIU, QAJYIL). In **MF** also an intramolecular $CH_2\cdots O1$ interaction is formed (C9H9B$\cdots$O1 distance: 2.353(4)Å; C9H9B$\cdots$O1 angle: 106.3(3)°) which we have speculated[4] could contribute to stabilize the *gauche* arrangement about C7-C8 by forming a five-membered ring. On the other hand, there is no doubt that the knowledge of the conformational space to which the pending side arm of metoprolol can have access is rather important, given that such a tail is common to a large variety of β-blockers drugs (*vide infra*). Considering the latter point, previous in silico studies[4] suggest that the three conformations adopted by the charged tail in the solid state represent stable and almost isoenergetic conformers (DFT data) separated by quite low energy barriers (molecular dynamics, MD, data). Besides the 2-hydroxy-3-isopropylaminopropoxy chain can adopt different conformations in response to different environments (MD simulations data in vacuum *vs* in simulated solvent; solid state data).[4]

Crystal Structure from X-Ray Powder Diffraction and Hirshfeld Surface Analysis

In the crystal lattice each metoprolol cation forms two strong[38] hydrogen bonds with two fumarate anions (symmetry related by the following screw axis: -x,y+1/2,-z-3/2) thanks to the ammonium group which acts as a double H-bond donor (Table 4, Figure 4). The hydroxyl group also contributes to reinforce one of the metoprolol-fumarate interaction working as H-bond donor, giving rise to a further strong interaction (Table 4); as a result, a nine-membered ring is formed which hold together this metoprolol-fumarate ionic couple (Figure 4). In particular the N1-H1BN···O5^{i} (^{i}=-x,y+1/2,-z-3/2) hydrogen bond can be categorized as a discrete pattern of D1,1(2)d type by using the graph set analysis implemented in Mercury,[39] while the couple of H-bonds N1-H1AN···O5&O2-H2O···O4 originates a ring of R2,2(9)>a<b type, that is a motif with 2 acceptors and 2 donors, which gives rise to a nine-membered ring (R) hold together by two non equivalent H-bonds (a,b code) involving the two ions.[40] Considering the fumarate anion, each carboxylate group H-bonds a metoprolol cation and gives rise to the already mentioned nine-membered ring. Due to symmetry reasons (the fumarate anion lies on a crystallographic inversion center), each anion (which is placed along the *c*-axis direction) bridges two opposite enantiomers of metoprolol as illustrated in Figure 5. In addition, because the fumarate O5 oxygen atom and its symmetry related O5^{ii} (^{ii}=-x, -y+1, -z-2) act as bifurcated acceptors, each of them bound a further metoprolol cation giving rise to a chain along the *b*-axis direction formed by alternating R and S cations bridged by the anion and bound through the D1,1(2)d type motif (Figure 5). In addition two weak CH···π contacts (Table 4) hold together couples of identical enantiomers along the *b* axis.

Given that most β-adrenergic agonist and antagonist drugs having a charged amine or ethanolamine tail interact with the receptor anchor site formed by the carboxylate groups of Asp113,[41] the CSD was searched for non-bonded intermolecular interactions between the fragments sketched in Scheme 2b. The search gives 20 hits: i) 8 of them show an R2,2(9) H-bond motif pattern between the interacting partners; ii) in 14 of them the carboxylate group belongs to a dicarboxylic acid and, in 6[35,42,43,4,19] of these, the ionic couple is held together by an R2,2(9) pattern as found in **MF**. In all of these latter salts the cation is a β-adrenergic drug: 3-((4-Acetyl-2-propoxymethyl)phenoxy)-2-hydroxypropyl)(isopropyl)amine,[43] atenolol,[35] propanolol[42] and metoprolol.[4,19]

In particular in all the metoprolol salts **(MF**, **MS-m**,[19] **MT-o**[4] and **MT-m**[16]), each cation is strongly H-bound to two counterions, while each anion acts as H-bond acceptor towards four metoprolol cation (2R and 2S). In addition the H-bond interactions in **MF**, **MS-m**[19] and **MT-o**[4,18] appear comparable in terms of distances and angles (Tables 4 and S1), the same applies for crystal densities and packing efficiencies, the latter evaluated as K.P.I.:[44,45] densities=1.22, 1.25, 1.24 g cm^{-3}; K.P.I.=0.67, 0.72, 0.67 for **MF**, **MS-m** and **MT-o**, respectively. In addition to the already pointed out R2,2(9)>a<b type motif,[39] also the D1,1(2) motif is common to these three solids;

however in **MF** and **MT-o** it gives rise to metoprolol-dicarboxylate chains, while in **MS-m** it is part of two ring motifs (R4,4(12)>b<c>b>c and R2,4(14)>a<c>a>c) which comprise a couple of R/S metoprolol cation and two succinate anions (Figure S2). [39]

The Hirshfeld surface (HS) analysis was then used to further investigate the intermolecular interactions which held together **MF**, **MS-m** and **MT-o** in their respective solids. HSs for the metoprolol cation mapped with d_{norm} highlighting the intermolecular contacts are shown in Figures 6a-6b: in all cases the dominant interaction is related to the R2,2(9) motif (two large red spots); the weaker NH···O interaction (D1,1(2) motif) as well as the less prominent contacts show up as pale red regions. The corresponding fingerprint plots are shown in Figure 7. All the fingerprints show a quite long and asymmetric spike at the bottom left of the plot which is associated to the NH/OH→O hydrogen bonds, while the two lateral wings (d_i, d_e ~ 2.0-2.4Å) can be largely attributed to the CH···π interactions. In all cases, the H···H hydrophobic contacts represent almost 2/3 of the intermolecular interactions of the metoprolol cation, as provided by the percentage contributions to the Hirshfeld surface areas for the different non-bonding interactions (see figures S3-S5 in the Supplementary material). As a whole the H···O contacts account for about the 23%, being the H-bond donor contribution largely prevalent (ca. 15%, figures S3-S5). Finally, about the 12% of the surface can be identified as H···C interactions.[46]

These data point out that the nature and contribution of the intermolecular contacts between the metoprolol cations and the corresponding dicarboxylate counterions, are very similar, e.g. they appear to play an almost identical role in the corresponding crystal packings.

Bulk behavior from Variable Temperature X-Ray Powder Diffraction and Differential Scanning Calorimetry

DSC measurements performed on **MF** in the 310-450K range do not evidence any thermal event (see Figure S6) except that related to the melting at around 422 K (peak 422.0 K, extrapolated peak 422.1 K) which has the highest enthalpy in the **MT-o**, **MS-m**,[47] **MF** series (180.7 J/g = 116.3 kJ/mol). Consistently with the DSC profile, the XRPD patterns measured in the temperature range 300-430K superimpose quite well (Figure 8): there are no changes in the overall number of the peaks and in their relative intensities on heating. Thus no phase transitions occur in these experimental conditions up to **MF** reaches the melting point (as already found for the **MT-o** and **MS-m** samples).[4] However, a closer inspection of the XRPD patterns shows that peaks shift to a different extent as temperature is increased: several peaks move towards lower 2ϑ, while the position of others remains almost unchanged, thus suggesting that an anisotropic thermal expansion takes place on increasing the temperature (as previously observed for **MS-m**).[4] In particular the

shift is evident for the (0k0), (hk0) and (0kl) peaks; by contrast, (h00), (00l) and (h0l) peaks do not move significantly with the temperature growth. The lattice parameters calculated from the XRPD patterns listed in Table 2 (details in the Experimental section) confirm this observation: the *b* axis significantly expands with respect to both the *a* and *c* axes which remain almost unchanged. This trend is well quantified by the linear thermal expansion coefficients (TECs)[48] listed in Table 5. Finally, similarly to the tartrate salt,[4] **MF** does not immediately recrystallize upon cooling; however, after three days the sample, left in air at room temperature, recovers its starting crystalline phase, as provided by the XRPD profiles shown in Figure S7.

In summary: i) the crystalline phase of the **MF** salt is stable from r.t. until melting begins (DSC and VT-XRPD data); ii) during the heating cycle the lattice expands anisotropically (VT-XRPD data); iii) the molten sample does not immediately recrystallize on cooling (VT-XRPD data); but it needs at least three days to revert to its starting crystalline phase (XRPD data).

DISCUSSION

The results above reported suggest that at the atomic level, e.g. when the molecular and crystal structures of **MF** are taken into consideration and compared to those of the strictly related **MS-m** and **MT-o** salts, the three solids appear at first sight almost identical. For example the overall shape adopted by the metoprolol cation in the fumarate salt well superimposes with that found in **MS-m** and both are almost isoenergetic with that found in **MT-o** (DFT data).[4] In addition the strongest H-bonds which hold together the crystal structures of **MF**, **MS-m** and **MT-o** are characterized by very similar bond distances and angles (Table 4 and S1) and, more interestingly, they describe identical motifs; finally even the contributions to the Hirshfeld surfaces of the different intermolecular contacts are comparable. Consistently densities and K.P.Is. are almost the same for the three salts.

However as already noticed for the **MT-o** and **MS-m** case,[4] these similarities do not imply similar macroscopic behavior and thus highlight the difficulty in correlating structural aspects at the atomic level with changes in physical properties.

Specifically, both melting enthalpies and temperatures increase in the series **MT-o**, **MS-m** and **MF** (ΔH_{max} ~ 16kJ/mol and ΔT_{max} ~ 27K), thus suggesting a growing cohesive force, whose trend however does not correlate with the corresponding density and K.P.I. values. In particular, in all cases melting occurs at a temperature comprised between the melting points of metoprolol (323K)[16] and of the related pure acids.[49] In particular, as already observed,[50,51,52] the melting points of the three salts follow the same trend as those of the corresponding pure acids. A similar relationship

between melting points of API cocrystals and cocrystal formers has also been reported,[53] but not always it has been fully rationalized.[54] In fact numerous factors can contribute to establish the melting point of a crystalline sample (e.g. molecular and crystal symmetry, intermolecular interactions,[55] conformational freedom), thus making it very difficult to find well-defined correlations between solid state arrangement and melting point.[56] In addition the molecular structure also can play a role in determining trends in melting temperatures. For example unfavourable molecular conformations driven by crystal packing requirements could contribute to lower the melting temperature as provided by Boese et al.[57] in a paper dealing with the melting point alternation in the series of the C2- to C10-diacids.

Besides both **MF** and **MS-m** undergo a reversible anisotropic lattice expansion/contraction upon temperature change, at variance with **MT-o** which expands/contracts isotropically upon temperature variation. In particular, both the fumarate and succinate salts expand significantly along the *b* axis direction, which is the unique axis in the monoclinic system (space group $P2_1/c$ and C2/c for **MF** and **MS-m**, respectively). However **MS-m** once melted quickly reverts to the starting crystal form, while the molten phase of both **MF** and **MT-o** gives an amorphous solid on cooling, which takes several days (at r.t.) to recrystallize to the starting phase.

Keeping this in mind we have reconsidered the crystal packing of the three metoprolol salts.

In **MT-o** the tartrate anions stack along the *c* axis direction with a little offset (Figure 9); as a result the hydroxyl oxygen atoms and the carboxylate groups belonging to contiguous anions are quite close to each others [$HO\cdots O^i$: 2.97(2) Å and $HO\cdots C^i$ 2.92(3) Å (i= -x+1,y,-z+1)].[58,59] Besides the conformation adopted by the C_4 chain (157(2)° /157(3)°) differs from the usually preferred *trans* one (CSD data).[6] By contrast in **MS-m** and **MF**, anions are not piled (Figure 10), but rather they intercalate through the metoprolol cations (in the succinate anion the dihedral angle about the central C-C bond has the canonical[6] *trans* arrangement). Thus we could speculate that, due to the packing, the tartrate anions adopt an unfavourable conformation which could contribute to lowering the melting temperature of **MT-o** with respect to **MS-m** and **MF**.

In addition, in both the fumarate and succinate salts, the rings originated by the R2,2(9) motifs are nearly parallel to the *ac* plane (Figure 11). As a consequence, varying the temperature, **MS-m** and **MF** expand/contract significantly only along the *b* axis, where the D1,1(2) H-bond motif is at work together with the weaker $CH\cdots\pi$ contacts between couples of identical enantiomers. By contrast in **MT-o** adjacent anions form H-bonded rings (R2,2(9) type) which are almost perpendicular to each other (Figure 12) and, as a result, there is not a preferred direction along which the crystal can expand/contract.

However we know that the crystal packing of these salts is the result of a complex interplay between interionic interactions, H-bondings, CH-π and van der Waals interactions and that it is difficult to draw really convincing correlations between molecular/crystal structure and thermal behavior (melting temperature/enthalpy; isotropic/anisotropic thermal expansion amorphous/crystalline transformation).

CONCLUSIONS

In this study the molecular and crystal structure of the metoprolol fumarate salt (MF), as determined from XRPD data, has been discussed and compared with those of the analogous tartrate (**MT-o**) and succinate (**MS-m**) salts. In addition the thermal behavior of **MF** has been studied by DSC and VT-XRPD measures.

We have found that: (a) the overall shape adopted by the metoprolol cation in the fumarate salt well superimposes with that found in MS-m; in addition previous studies suggest that the charged ethanolamine chain is quite flexible and it is able to change its conformation depending on the surrounding (CSD,[6] MD and QC data[4]); (b) the H-bond motifs which hold together the crystal structures of **MF**, **MS-m** and **MT-o** are very similar (Graph Set analysis); (c) consistently the contributions of the different intermolecular contacts are comparable (Hirshfeld Surface Analysis); d) densities and K.P.I. are almost the same for the three salts.

Notwithstanding these similarities **MF** (as **MS-m**) expands/contracts anisotropically, (but the melt takes three days to recover the starting crystalline phase, as **MT-o**) and the melting temperature and enthalpy regularly increase in the series **MT-o**, **MS-m** and **MF** suggesting increasing cohesive forces.

The accurate examination of their crystal arrangements shows that in **MT-o** there are piles of tartrate ions alternating with the metoprolol cation disposed along the *c* axis direction, whereas in **MS-m** and **MF** the metoprolol cations and the corresponding anions are interposed. This causes a different distribution of the R2,2(9) H-bond motif within the crystal (anisotropic in **MF** and **MS-m** *vs* isotropic in **MT-o**) which could account for their different thermal behavior (anisotropic *vs* isotropic thermal expansion/contraction). Moreover in the latter, the strained conformation of the stacked tartrate anions could contribute to lower its melting point.

Even if it should be made clear that correlations relating solid state structures to physicochemical properties remain elusive, still we believe that a thorough solid state characterization can offer crucial information especially when dealing with APIs.

Author Contributions

The manuscript was written through contributions of all authors. All authors have given approval to the final version of the manuscript.

Acknowledgment

Authors thank the Centro di Cristallografia Strutturale (CRIST) of the University of Florence for the X-ray diffraction facilities and Dr. Samuele Ciattini for his valuable technical assistance. In addition, thanks go to Dr Andrea Ienco (ICCOM-CNR, Florence) and Prof. Lucia Maini (University of Bologna) for their technical help.

Table 1: Crystallographic data and refinement parameters for **MF**.

Formula	$C_{34}H_{54}N_2O_{10}$
MW	648.80
T (K)	298
λ (Å)	1.54056
Crystal system, space group	Monoclinic, $P2_1/c$
Unit cell dimensions (Å, °)	a = 13.3415(6) b = 8.2859(4); β = 108.74(2) c = 17.0030(7)
Volume ($Å^3$)	1779.9(1)
Z, D_c (mg/cm^3)	2, 1.218
μ (mm^{-1})	0.698
R_{wp} (%)	4.07
GOF's	2.316

Table 2. Cell parameters for **MF** at different temperatures from XRPD data.

T(K)	*a(Å)*	*b(Å)*	*c(Å)*	*β(°)*	V*(Å^3)*	Rwp
298	13.392(1)	8.316(1)	17.066(7)	108.81(1)	1799.1(8)	5.78
310	13.3947(9)	8.335(1)	17.071(6)	108.84(1)	1803.6(7)	5.95
320	13.3970(9)	8.346(1)	17.079(6)	108.84(1)	1807.2(1)	5.76
330	13.3990(9)	8.358(1)	17.088(6)	108.87(1)	1810.9(7)	5.73
340	13.4010(9)	8.374(1)	17.087(5)	108.90(1)	1814.2(6)	5.68
350	13.4036(8)	8.390(1)	17.088(5)	108.93(1)	1817.7(6)	5.74
360	13.4075(8)	8.408(1)	17.069(5)	108.97(1)	1819.8(6)	5.69
370	13.4095(8)	8.426(1)	17.069(5)	108.99(1)	1823.7(6)	6.00
390	13.4149(8)	8.465(1)	17.075(5)	109.00(1)	1833.3(6)	6.05

Table 3. Main torsion angles (°), obtained from X-ray diffraction studies, defining the overall shape of the S enantiomer of metoprolol cations in **MF**, **MS-m**[a] and **MT-o**[b].

Torsion angle[a]	**MF**	**MS-m**[a]	**MT-o**[b]
C(6)-C(1)-O(1)-C(7)	-172.8(2)	-178.9[c]	-169
C(1)-O(1)-C(7)-C(8)	-175.5(2)	-177.6	167
O(1)-C(7)-C(8)-C(9)	-56.2(3)	-65.1	-174
C(7)-C(8)-C(9)-N(1)	164.4(3)	166.9	156
C(8)-C(9)-N(1)-C(10)	-178.3(4)	172.0	176
C(9)-N(1)-C(10)-C(11)	-168.1(5)	177.5	166
C(9)-N(1)-C(10)-C(12)	68.6(6)	54.1	-61
C(3)-C(4)-C(13)-C(14)	-136.4(6)	-128.7[d]	-96
C(4)-C(13)-C(14)-O(3)	-177.5(6)	175.1	-173
C(13)-C(14)-O(3)-C(15)	-136.4(6)	-170.6	-174

[a] Values from ref. 19.

[b] Values from ref. 4.

[c] Value refers to the C(2)-C(1)-O(1)-C(7) in 19.

[d] Value refers to the C(5)-C(4)-C(13)-C(14) in 19.

Table 4. Selected Intermolecular Interactions in **MF**.

Strong H-Bonds			
D-H···A	D···A (Å)	H···A (Å)	X-H···A (°)
N(1)-H(1AN)…O(5)	2.79(1)	1.90(1)	162.0(8)
N(1)-H(1BN)…O(5)^{i}	2.76(2)	1.86(2)	165.9(5)
O(2)-H(2O)···O(4)	2.71(1)	1.91(1)	161.3(7)
Weak interactions			
	H···C_T (Å)	C-H···C_T (°)	H···CT/$(C_1\text{-}C_6)_{\text{mean plane}}$(°)
C(13)-H(13B)···C_T^{ii}	2.955(8)	157.29(1)	81.7(1)
C(14)-H(14B)···C_T^{iii}	3.132(8)	156.54(2)	84.5(1)

^{i} = -x,y+1/2,-z-3/2

^{ii} = -x+1,y+1/2,-z-1/2

^{iii} = -x+1,y-1/2,-z-1/2

Table 5. Linear (α) and volume (β) thermal expansion coefficients (TECs)[48] calculated for **MF** taking as reference the cell parameter values calculated at 298K.

T(K)	$\alpha a(10^{-5})\,C^{-1}$	$\alpha b(10^{-5})\,C^{-1}$	$\alpha c(10^{-5})\,C^{-1}$	$\beta(10^{-4})\,C^{-1}$
298				
310	1.3	19.0	1.9	1.7
320	1.5	16.4	3.0	1.8
330	1.5	15.8	3.7	1.9
340	1.5	16.6	2.7	1.9
350	1.6	17.1	2.3	1.9
360	1.8	17.8	0.3	1.8
370	1.7	18.4	0.2	1.8
390	1.8	19.5	0.5	2.0

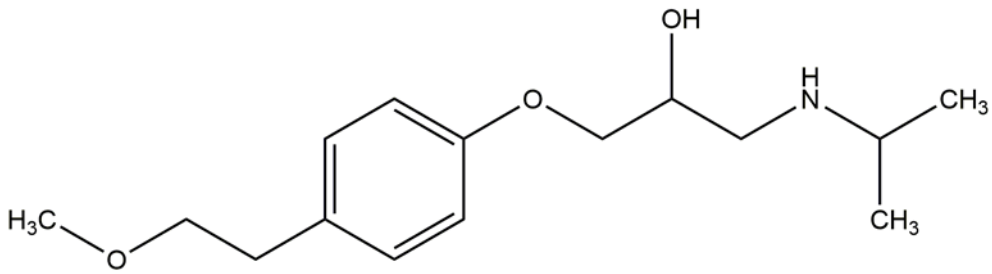

Scheme 1. Schematic drawing of the metoprolol molecule.

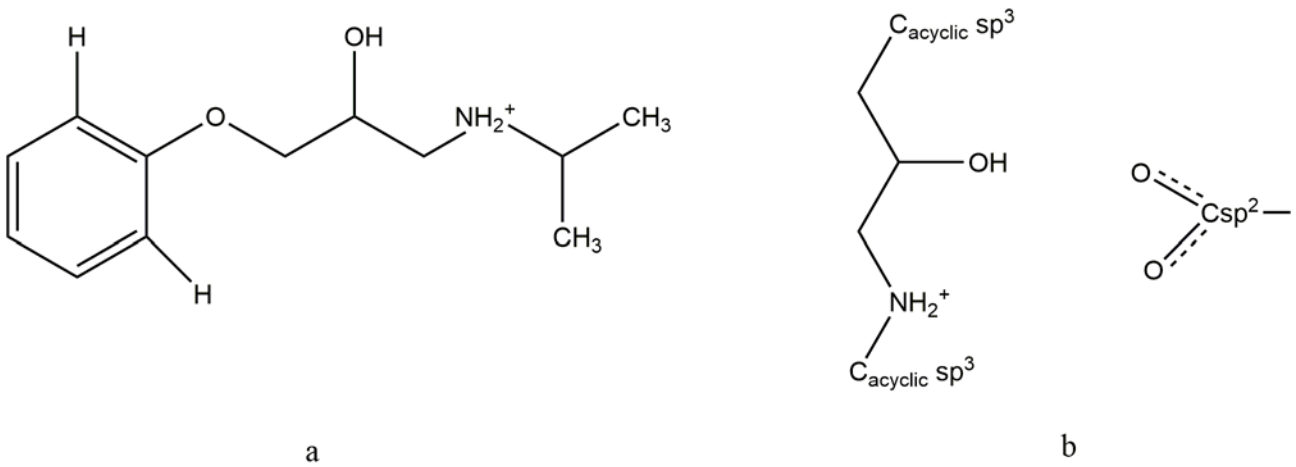

Scheme 2. Fragments searched in the CSD (see text for details).

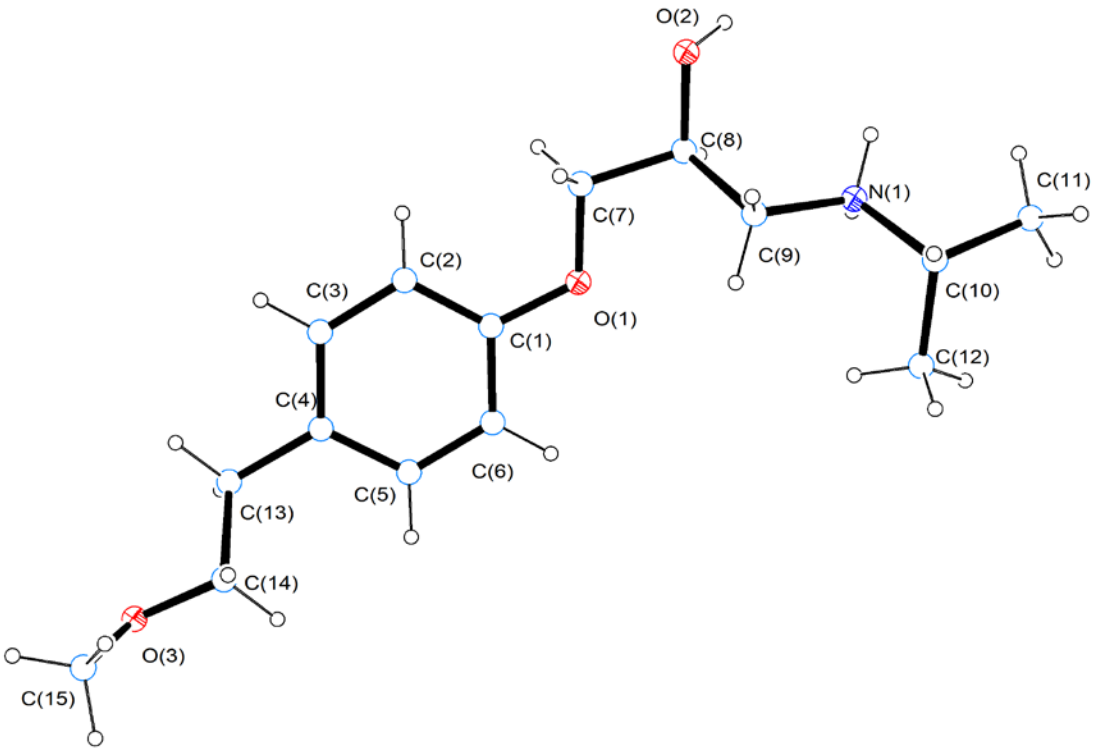

Figure 1. ORTEP-3 view of the S enantiomer of metoprolol cation in **MF** (ellipsoid probability 20%).

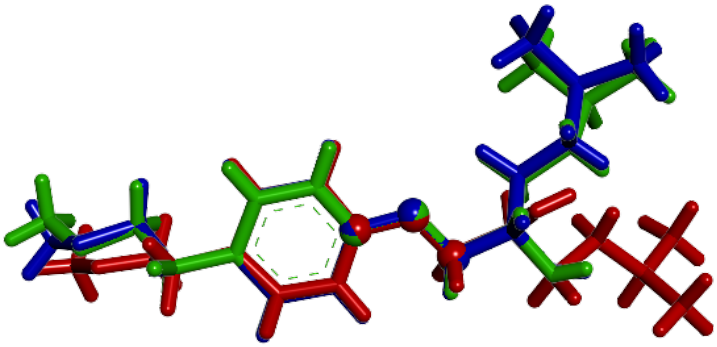

Figure 2. Superimposition of the X-ray structures of the S isomer of the metoprolol cation as found in **MF**, **MT-o** (ZUYJOU refcode in CSD) and **MS-m** (YOTXOV refcode in CSD). Structures are superimposed by "ball-and stick" atoms. Color key: **MF** = dark blue; **MS-m** = green; **MT-o** = red.

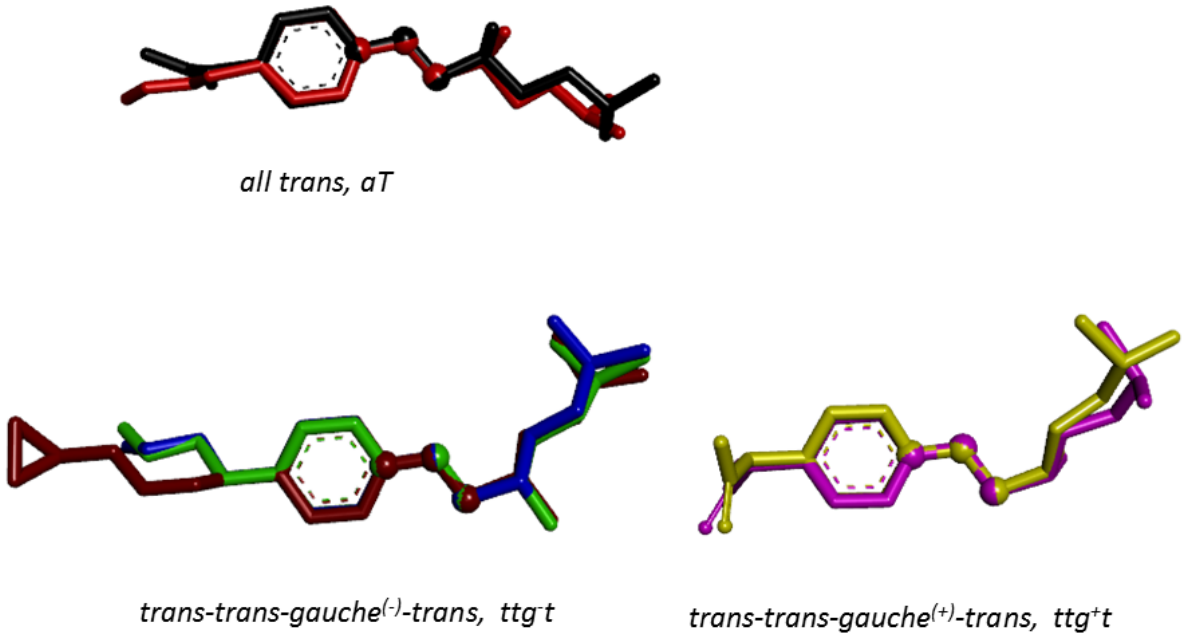

Figure 3. Superimposition of the X-ray structures of the S isomer of the metoprolol cation found in the CSD, plus **MF**. Structures are superimposed by "ball-and stick" atoms. Hydrogen atoms have been omitted for clarity. Color key: **MF**= dark blue, **MS-m** = green; **MT-o** = red, CIMJUD=brown, DETHIEU=yellow, JIRWIR=black, QAJYIL=purple.

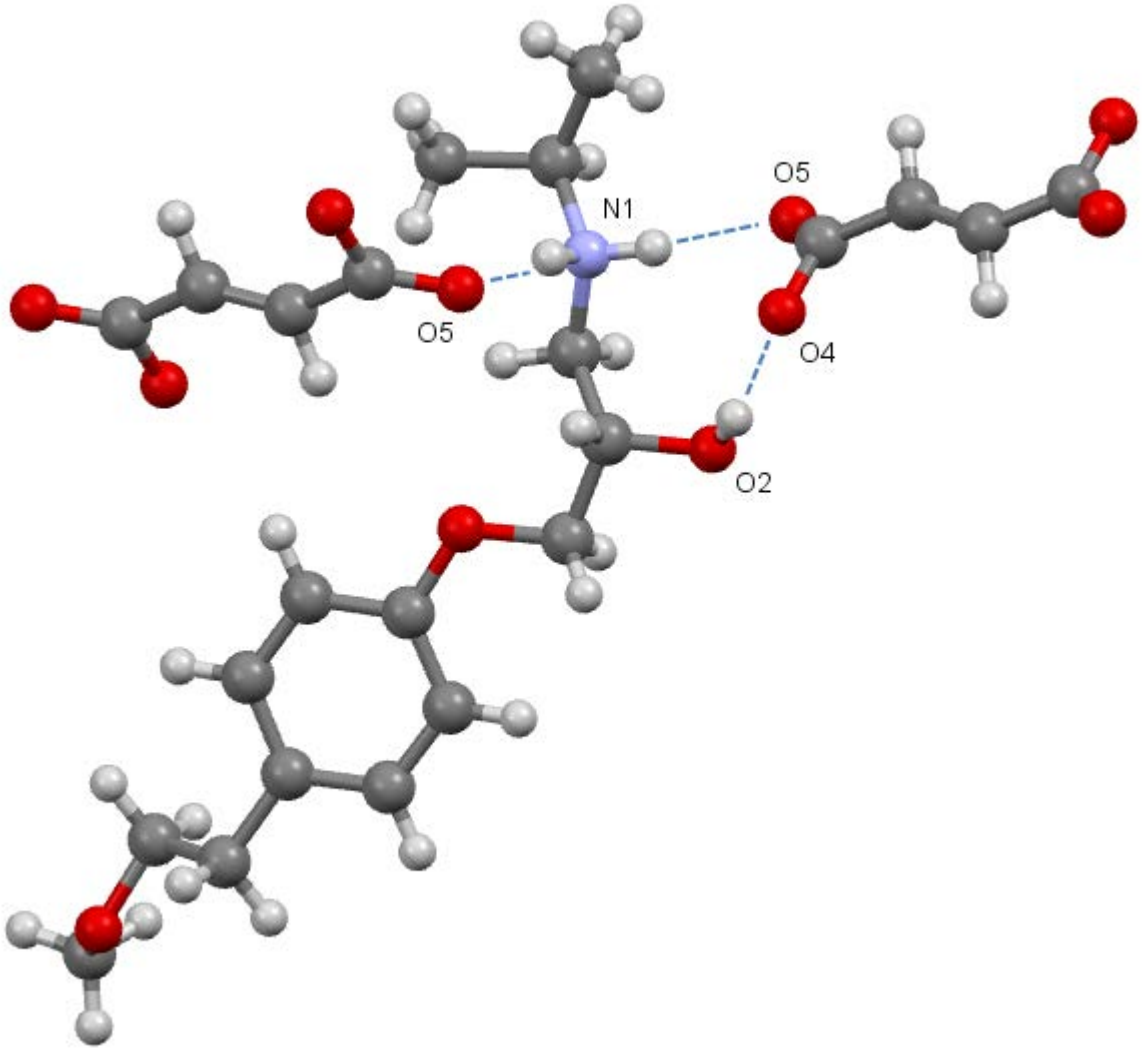

Figure 4. View of the net of H-bonds which holds together the metoprolol cation and two symmetry related fumarate anions in the crystal lattice. (Left: the H-bond categorized as D1,1(2)d; right: the ring motif of R2,2(9)>a<b type).

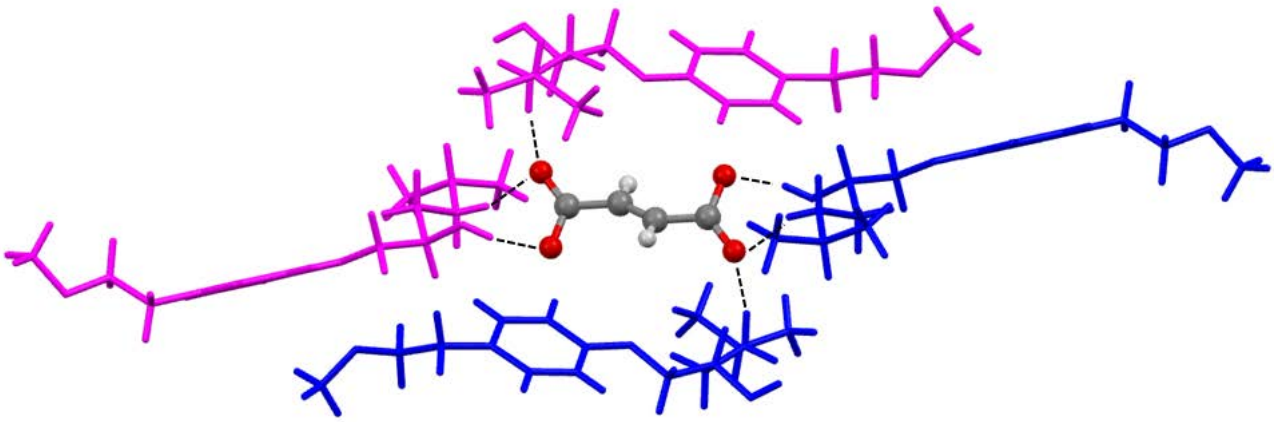

Figure 5. View of the net of H-bonds which hold together metoprolol and fumarate ions in the crystal lattice: each fumarate H-bonds four metoprolol cation (S and R enantiomers have different color).

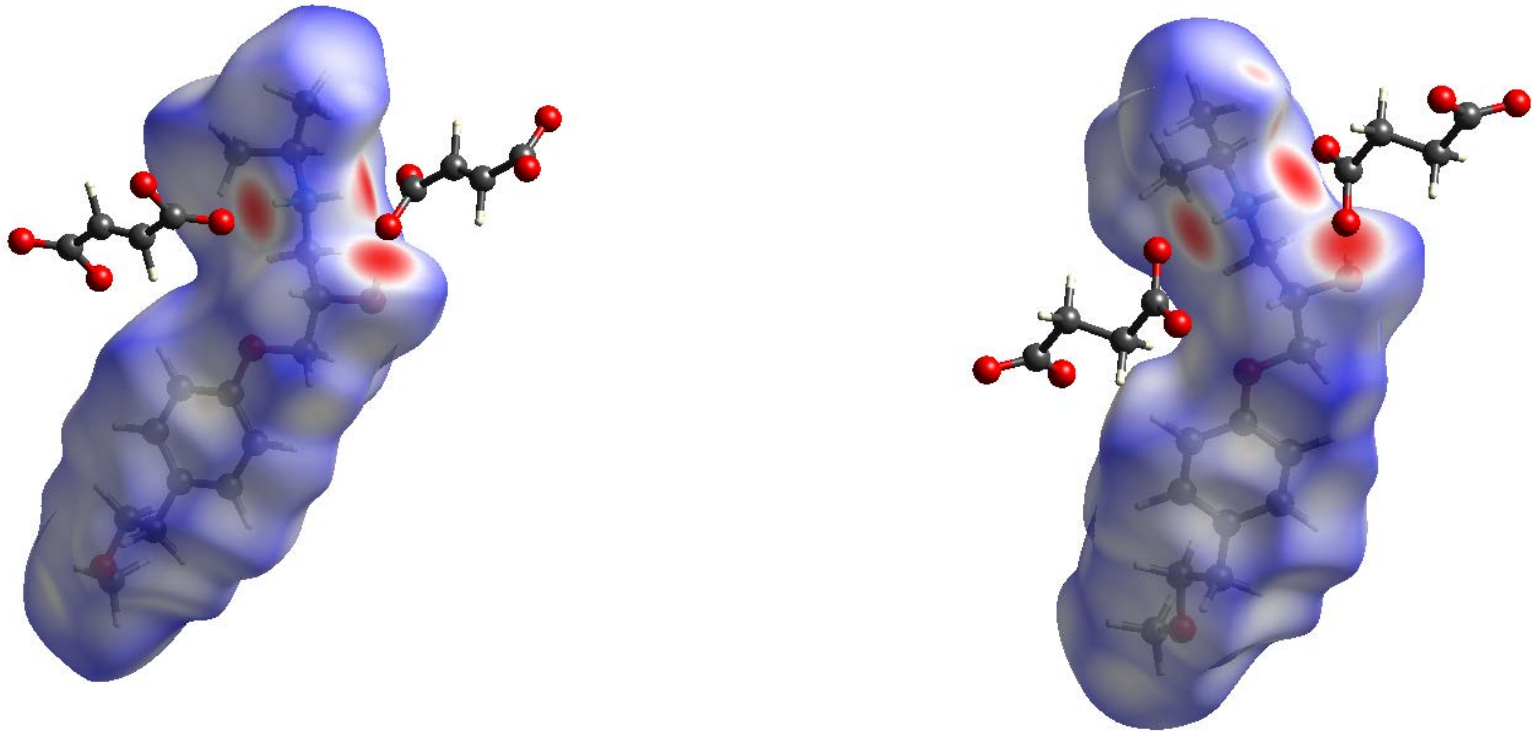

Figure 6a. d_{norm} surfaces of the metoprolol cation in the **MF** (left) and **Ms-m** (right) crystal lattices. Neighboring counterions associated with close contacts are also shown.

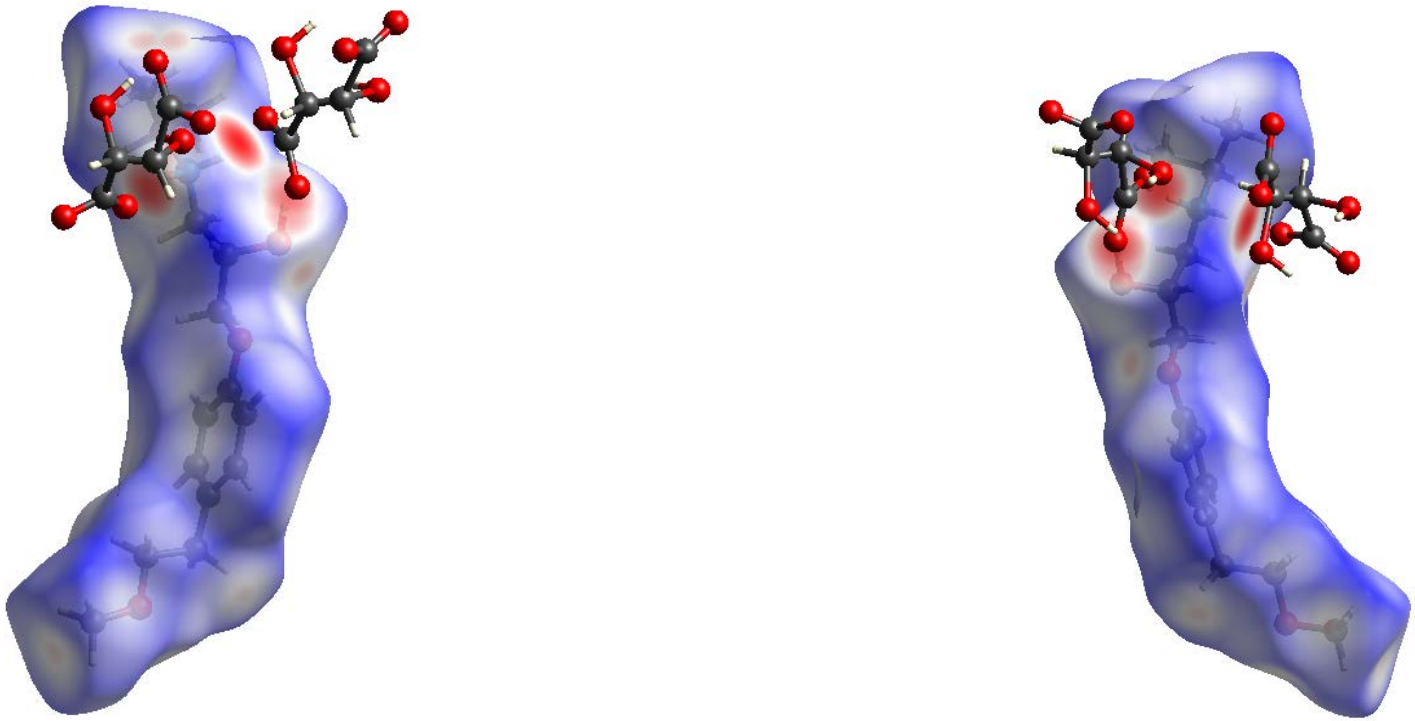

Figure 6b. d_{norm} surfaces of the two independent metoprolol cations (S on the left, R on the right) in the **MT-o** crystal lattices. Neighboring tartrate anions associated with close contacts are also shown.

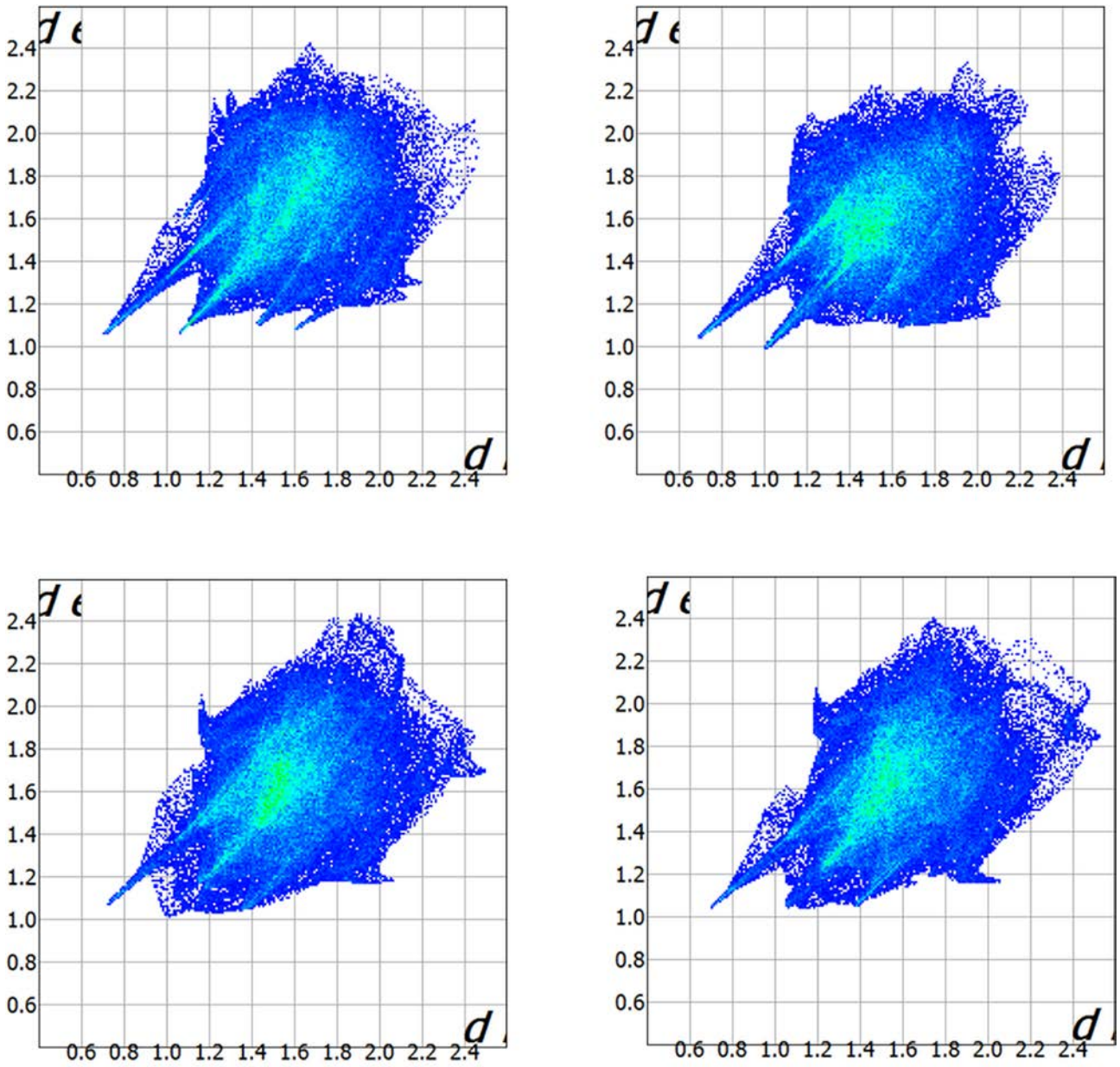

Figure 7. Fingerprint plots for the metoprolol cation in **MF** (up left), **MS-m** (up right) and **MT-o** (bottom, S and R enantiomer on the left and on the right, respectively).

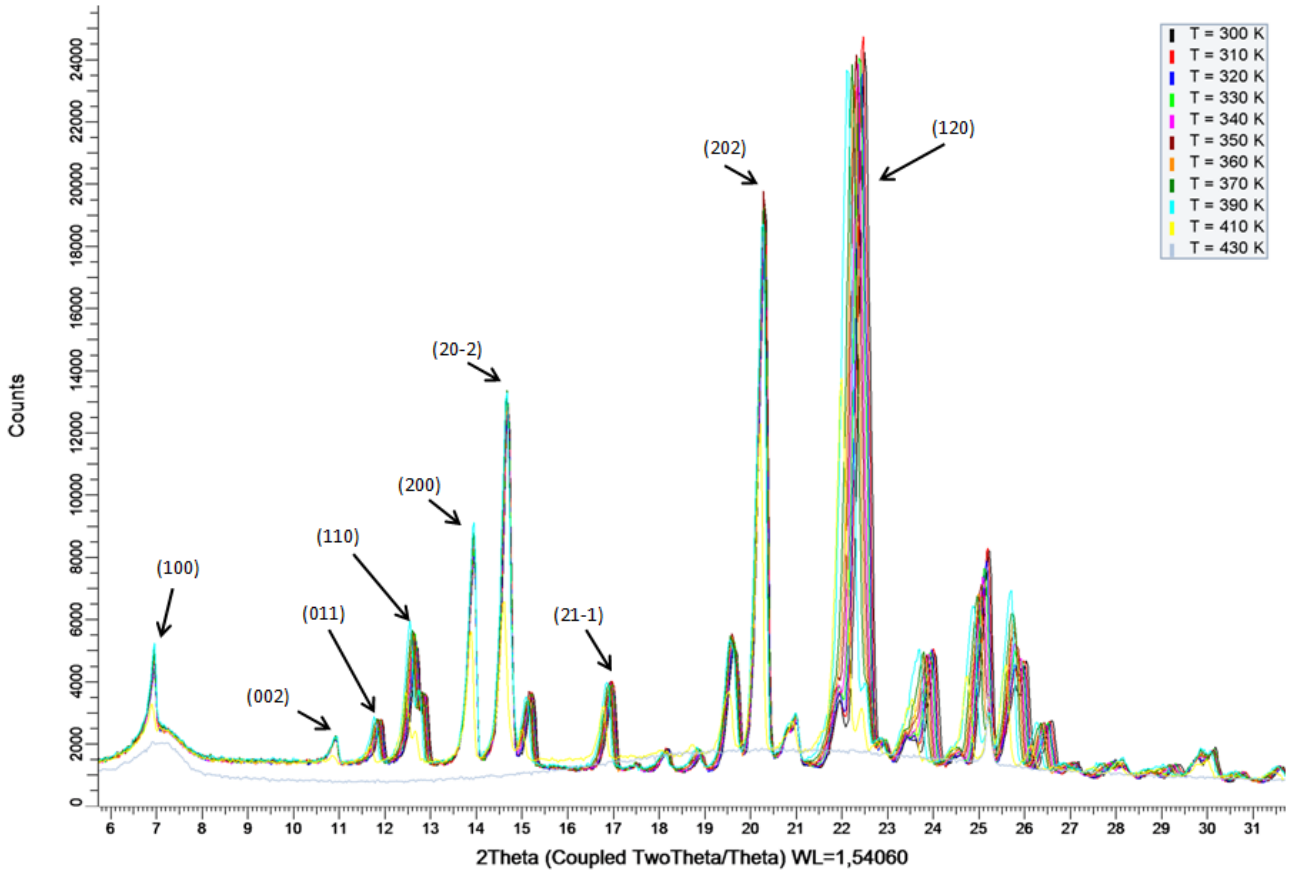

Figure 8. Superimposition of XRPD patterns of **MF** collected in the 300-430 K range.

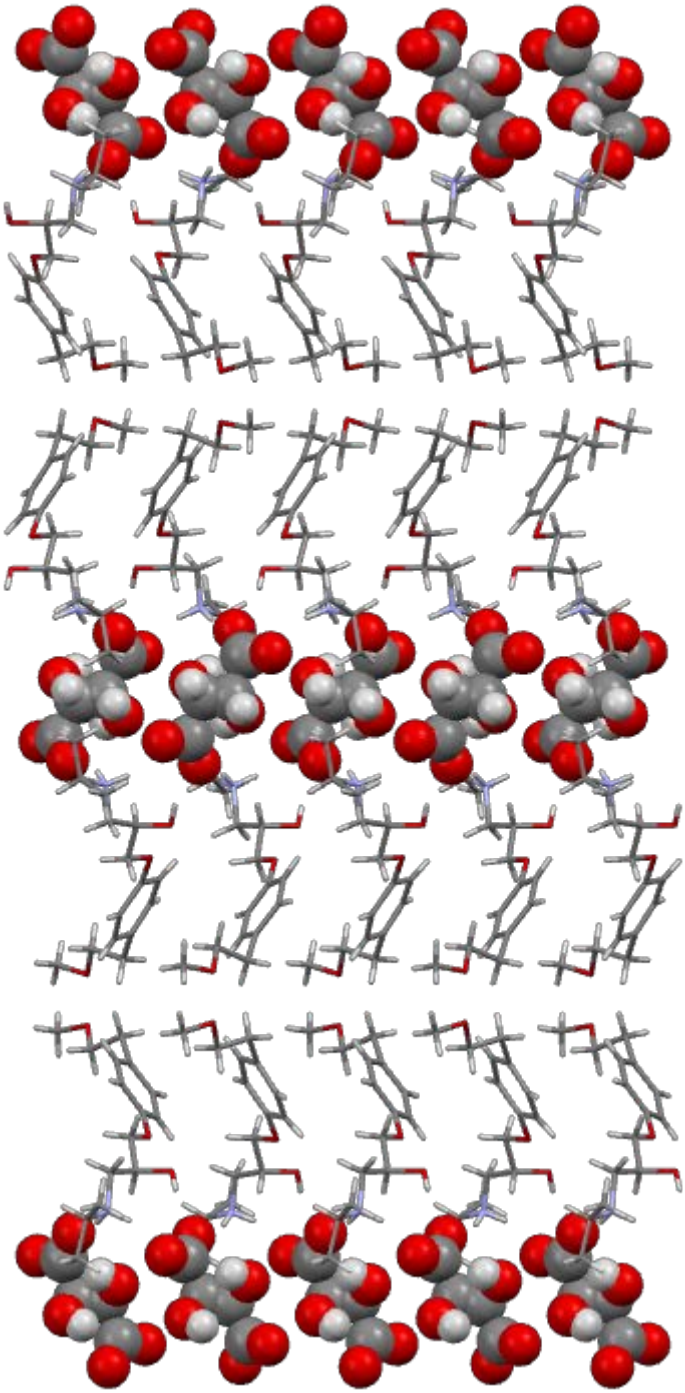

Figure 9. Crystal packing of **MT-o** (view along the *b* axis direction) highlighting the stacking of the tartrate anions (spacefilling) along the *c* axis direction.

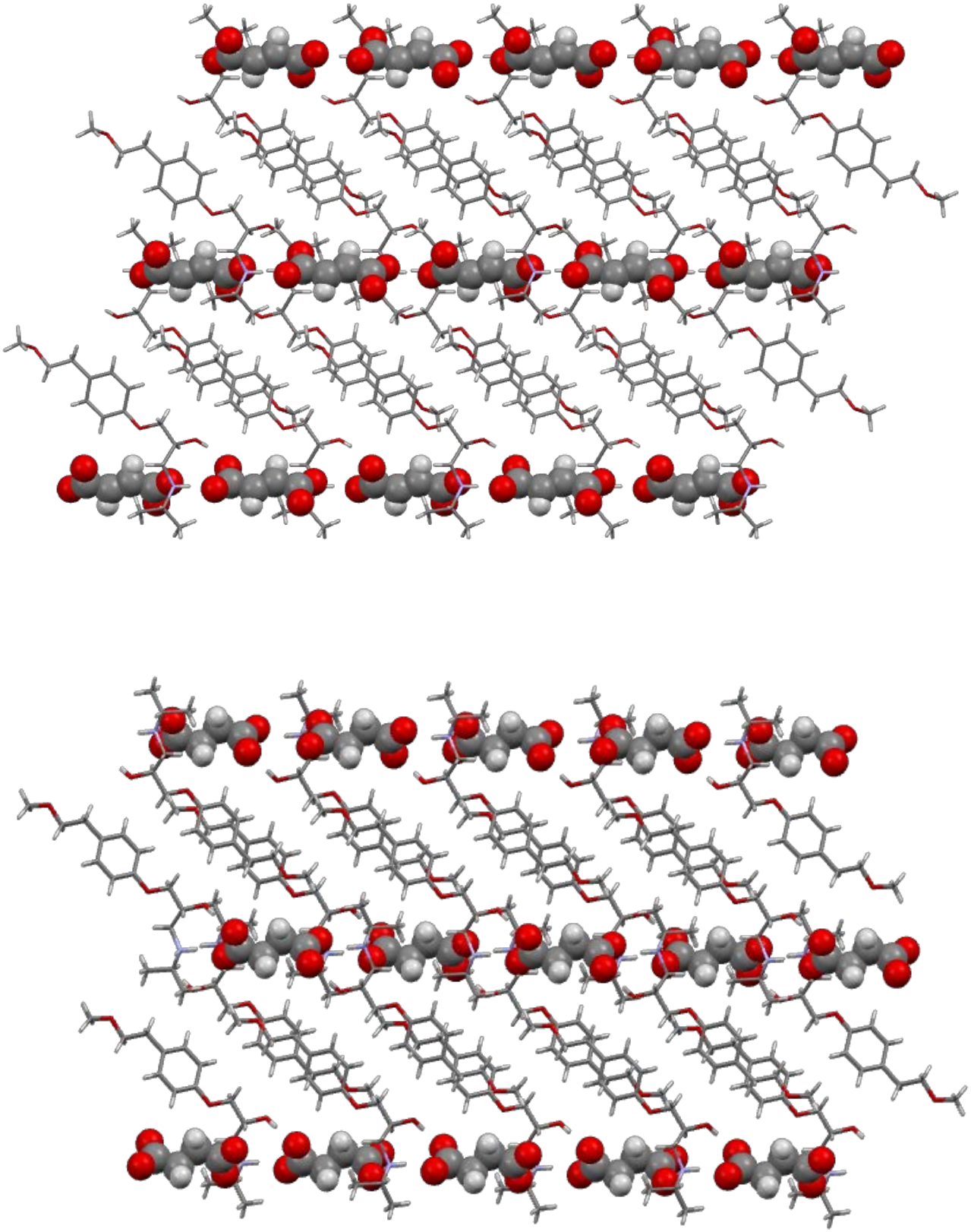

Figure 10. Crystal packings of **MF** (top) and **MS-m** (bottom) view along the *b* axis direction.

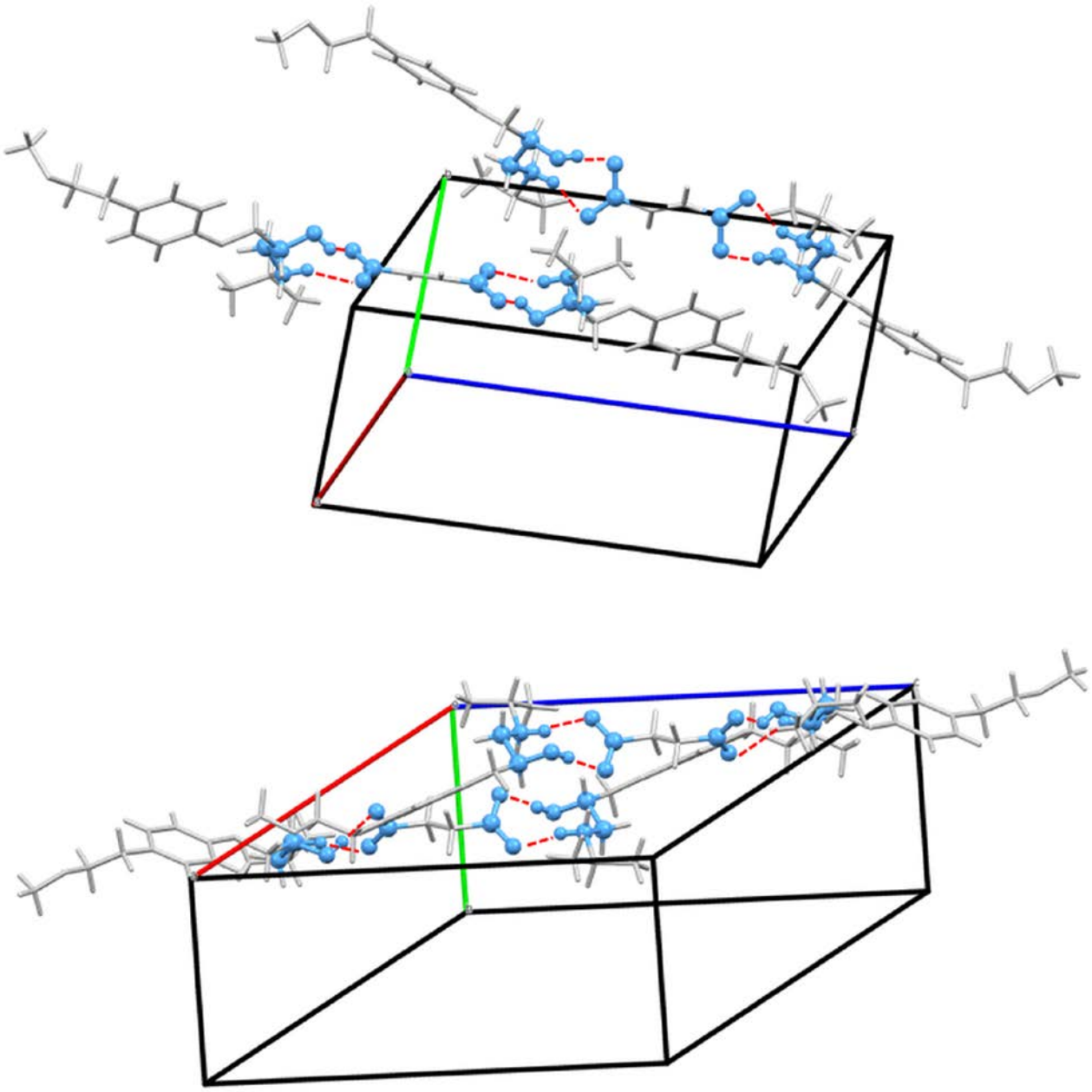

Figure 11. R2,2(9)>a<b ring motif in **MF** (top) and **MS-m** (bottom).

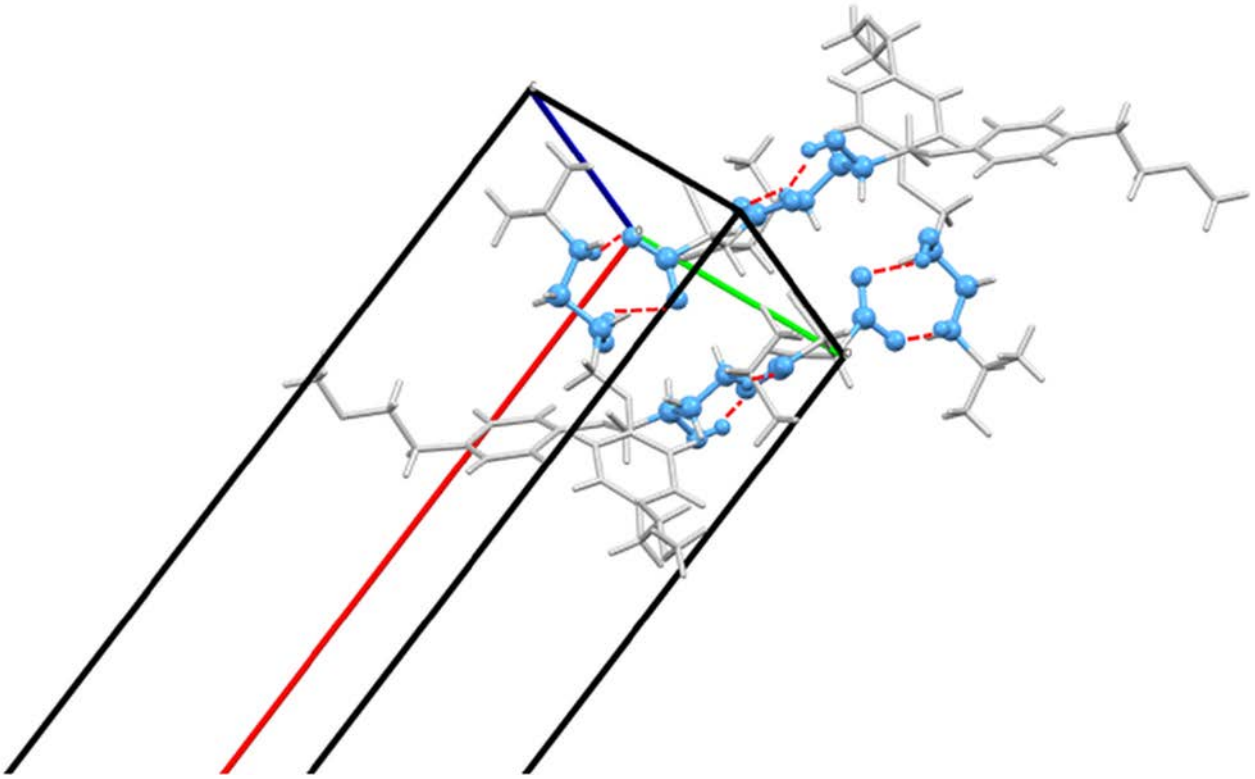

Figure 12. R2,2(9)>a<b ring motif in **MT-o**.

[1] *Solid State Characterization of Pharmaceuticals*, First Edition. Edited by Richard A. Storey and Ingvar Ymen, **2011** Blackwell Publishing Ltd.

[2] Bond, A. D.*Resonance* **2014**, *19*, 1087–1092.

[3] Rossi, P.; Macedi, E.; Paoli, P.; Bernazzani, L.; Carignani, E.; Borsacchi, S.; Geppi, M. *Crystal Growth and Design* **2014**, *14*, 2441-2452.

[4] Paoli, P.; Rossi, P.; Macedi, E.; Ienco, A.; Chelazzi, L.; Bartolucci, G.L.; Bruni, B. *Crystal Growth and Design* **2016**, *16*, 789-799.

[5] Paoli, P.; Rossi, P.; Chelazzi, L.; Altamura, M.; Fedi, V.; Giannotti, D. *Crystal Growth and Design* **2016**, *16*, 5294-5304.

[6] Groom, C. R.; Bruno, I. J.; Lightfoot ,M. P.; Ward, S. C. *Acta Cryst.* **2016**, *B72*, 171-179.

[7] Cambridge Structural Database Entry summary statistics, 5 January 2018.

[8] He, Q.; Zhu, J.; Gomaa, H.; Jennings, M.; Rohani, S. J. *Pharm. Sci.* **2009**, *98*, 1835−1844

[9] Giron, D. *J. Therm. Anal. Calorim.* **2002**, *68*, 335−357.

[10] Paluch, K. J.; Tajber, L.; Elcoate, C. J.; Corrigan, O. I.; Lawrence, S. E.; Healy, A. M. *J. Pharm. Sci.* **2011**, *100*, 3268−3283.

[11] Lee, E. H.; Smith, D. T.; Fanwick, P. E.; Byrn, S. R. *Cryst. Growth Des.* **2010**, *10*, 2314−2322.

[12] Moses, J. W.; Borer, J. S. *DM, Dis.-Mon.* **1981**, *27*, 1−61.

[13] Benfield, P.; Clissold, S. P.; Brogden, R. N. *Drugs* **1986**, *31*, 376−429.

[14] Brogden, R. N.; Heel, R. C.; Speight, T. M.; Avery, G. S. *Drugs* **1977**, *14*, 321−348.

[15] Dasbiswas, A.; Shinde, S.; Dasbiswas, D. *J. Indian Med. Assoc.* **2008**, *106*, 259−262.

[16] Ionescu, C.; Caira, M. R.; Bojita, M. T.; Nassimbeni, L. R.; Mhlongo, W. T. *Farmacia* **2006**, LIV, 9−17.

[17] Wikstrand, J.; Andersson, B.; Kendall, M. J.; Stanbrook, H.; Klibaner, M. *J. Cardiovasc. Pharmacol.* **2003**, *41*, 151−157.

[18] A second polymorph of **MT** (monoclinic crystal system) is known which crystal data are not deposited into CSD (Ionescu at al., ref 16).

[19] Bartolucci, G.; Bruni, B.; Coran, S. A.; Di Vaira, M. *Acta Crystallogr., Sect. E: Struct. Rep. Online* **2009**, *65*, o1364.

[20]More recently a new phase for **MS** has been identified by Zhou et al. (ref.21) on the basis of the XRPD diffraction pattern (but no further structural details are given).

[21] Zhou, M.; Ao, J.; Liu, S.; Wu, C.; Lai, A.; Gao, H.; Zhang, G. *Pharm. Dev. and Technol.* **2017**, *22*, 58-62.

[22]Etter, M.C.; MacDonald, J.C.; Bernstein, J. *Acta Crystallogr* **1990**, *B46*, 256-262.

[23] Turner, M. J.; McKinnon, J. J.; Wolff, S. K.; Grimwood, D. J.; Spackman, P. R.; Jayatilaka, D.; Spackman, M. A. CrystalExplorer17, **2017**, University of Western Australia.

[24] Boultif, A.; Louer, D. *J. Appl. Crystallogr.* **2004**, *37*, 724−731.

[25] Altomare, A.; Cuocci, C.; Giacovazzo, C.; Moliterni, A.; Rizzi, R.; Corriero, N.; Falcicchio, A. *J. Appl. Crystallogr*. **2013**, *46*, 1231−1235.

[26] Hosomi, H.; Ito, Y.; Ohba, S. *Acta Cryst., Sect C: Organic Compound* **1998**, *54*, 142-145.

[27] Coelho, A. Topas-Academic v.5, **2012**.

[28] STAR^e, Thermal Analysis Software. Mettler - Toledo Int. Inc – Sonnenbergstrasse 74 – CH-8603 Schwerzenbahc, Switzerland.

[29] Macrae, C. F.; Bruno, I. J.; Chisholm, J. A.; Edgington, P. R.; McCabe, P.; Pidcock, E.; Rodriguez-Monge, L.; Taylor, R.; van de Streek, J.; Wood, P. A. *J. Appl. Cryst.*, **2008**, *41*, 466-470.

[30] In **MS-m** the metoprolol cation is affected by disorder. However given the relative contribution of the two models used to account for the disorder (occupancy factor of 0.91 and 0.09) we thought anyway significant to compute the HS.

[31] The following dihedral angles were taken into account to define the arrangement of the side chain: C6-C1-O1-C7, C1-O1-C7-C8, O1-C7-C8-C9 and C7-C8-C9-N1, while the conformation about the final C9-N1 and N1-C10 bonds was neglected.

[32] In the asymmetric unit of **MT-m** four independent cations of metoprolol (2 R and 2 S) are present. As reported by Ionescu and co- workers (ref. 16), the conformations adopted by the two R, as well as those of the two S cations are comparable and very similar to those found in **MT-o** (ref. 4).

[33] Pascard, C.; Tran E.; Dau, H.; Manoury, P.; Mompon, B. *Acta Crystallogr., Sect.C: Cryst. Struct. Commun.*, **1984**, *40*, 1430-1432.

[34] Wang, E.-J.; Chen, G.-Y. *Acta Crystallogr., Sect. E: Struct. Rep. Online*, **2011**, *67*, o91.

[35] Cai, J.; Liu, P.-D.; Ng, S. W. *Acta Crystallogr., Sect.E: Struct. Rep. Online*, **2006**, *62*, o5532-o5533.

[36] Lou, B.; Boström, D.; Velaga, S.P. *Acta Crystallogr., Sect. C: Cryst.Struct.Commun.*, **2007**, *63*, o714-0716.

[37] Conformers were grouped neglecting differences about the final C9−N1 and N1−C10 bonds.

[38] Desiraju G. R., Steiner T., *The weak hydrogen bond*, **1999,** IUCr Monographs on Crystallography, Oxford Science Publications

[39] Motherwall, W.D.S.; Shields, G.P.; Allen F.H. *Acta Cryst.*, **2000**, *B56*, 466-473.

[40] Bernstein, J.; Davis, R.E.; Shimoni, L.; Chang, N.-L. *Angew. Chem. Int. Ed. Engl*. **1995**, *34*, 1555-1573.

[41] Strader C.D.; Sigal, I.S.; Candelore, M.R.; Rands, E.; Hill, W.S.; Dixon, R.A. *J. Biol. Chem.*, **1988**, *263*, 10267-10271.

[42] Stepanovs, D.; Jure, M.; Yanichev, A.; Belyakov, S.; Mishnev, A. *CrystEngComm* **2015**, *17*, 9023-9028.

[43]Kettmann, V.; Dillinger, J.; Cizmarikova, R. *Acta Crystallogr.,Sect.C:Cryst.Struct.Commun.* 1991, **47**, 570-573.

[44] Kitaigorodskii, A. I. Organic Chemical Crystallography; Consultants Bureau: New York, 1961; pp 106−110.

[45] Calculated by using PLATON, A Multipurpose Crystallographic Tool; Spek, A.L., Utrecht University: Utrecht, The Netherlands, **1998**.

[46] The HSs for the anions show all the interactions described above (Figure S8); the fingerprint plot of all the anion shows an asymmetric spike at the bottom left of the plot, associated with the carboxylate acceptor (O←NH/OH hydrogen bond). As expected in all cases (Figures S9-S12) the O···H contacts represent the largest contributions (61-69%), followed by the H···H hydrophobic ones (24-34%). While they differ for the contribution of the C···H contacts (12.5% for fumarate, about 2% for the other two anions) and of the O···O ones (about 3% in the tartrate anions, negligible for the others).

[47] **MT-o** melting temperature: peak = 394.7 K, extrapolated peak 394.7 K; melting enthalpy 155.6 J/g, 106.5 kJ/mol from ref. 4; **MS-m** melting temperature: peak = 410.4 K, extrapolated peak 410.8 K; melting enthalpy 175.4 J/g, 114.4 kJ/mol from ref. 4.

[48] TECs = $\alpha = \frac{1}{l}_{T=0} \cdot \frac{\Delta l}{\Delta T}$ and $\beta = \frac{1}{V}_{T=0} \cdot \frac{\Delta V}{\Delta T}$, see: a) Hori, R.; Sugiyama, J.; Wada, M. *Carbohydrate Polymers*, **2007**, *70*, 298-303; b) Krishnan, R. S.; Srinivasan, R.; Devanarayanan, S. *Thermal Expansion of Crystals*, Pergamon, 1979.

[49] D-tartaric acid melting point: 441-443K; succinic acid melting point: 457-459K; fumaric acid melting point 572-573K; in Clayden J., Greeves N.; Warren S., Wothers P. *Organic Chemistry*, **2001**, Oxford University Press.

[50] Braga, D; Chelazzi, L.; Grepioni, F.; Dichiarante, E.; Chierotti, M. R.; Gobetto, R. *Crystal Growth & Des*., **2013**, *13*, 2564-2572.

[51] de Moraes, L. S.; Edwards, D.; Florence, A.J.; Johnston, A.; Johnston, B.F.; Morrison,C.A.; Kennedy, A.R. *Cryst Growth Des* **2017**, *17*, 3277– 3286.

[52] Galcera, J.; Molins, E. *Cryst Growth Des* **2009**, *9*, 327– 334.

[53] Schultheiss, N.; Newman, A. *Cryst Growth Des* **2009**, *9*, 2950– 2967.

[54] Friščić, T.; Jones, W.; *J. Pharm Pharmac.* **2010**, *62*, 1547-1559.

[55] Lemmerer, A.; Bourne, S.A. ; Fernandes, M.A. *CrystEngComm*, **2008**, *10*, 1605-1612.

[56]Katritzky, A. R.; Jain, R.; Lomaka, A.; Petrukhin, R.; Maran, U.; Karelson, M. *Cryst. Growth Des.* **2001**, *1*, 261–265.

[57] Thalladi, V.R.; Nüsse, M.; Boese, R. *J. Am. Chem. Soc.* **2000**, *122*, 9227-9236.

[58] The sum of the corresponding Van der Waals radii (from. ref. 58) is 3.04Å (O···O) and 3.22Å (C···O).

[59] Bondi A. *J. Phys. Chem*., **1964**, *68*, 441-451.